Grazer-induced bioluminescence and toxicity in marine dinoflagellates

Paula Gonzalo-Valmala[1](ORCID: 0009-0005-4270-4860)**, Milad Pourdanandeh**[2] (ORCID: 0009-0002-7640-5728), **Sandra Lage**[3] (ORCID: 0000-0003-0167-7163)**, Erik Selander**[1*] (ORCID: 0000-0002-2579-0841)

[1] Department of Biology, Lund University, Lund, Sweden

[2] Department of Marine Sciences, University of Gothenburg, Gothenburg, Sweden

[3] Centre of Marine Sciences (CCMAR/CIMAR LA), University of Algarve, Faro, Portugal

*** Correspondence:**

Name: Erik Selander

E-mail: erik.selander@biol.lu.se

Running head: Grazer-induced responses in marine dinoflagellates

Keywords: Marine dinoflagellates, Inducible defenses, Copepods, Copepodamides, Bioluminescence, Harmful algae, Paralytic shellfish toxins

Significance statement

Zooplankton grazers induce defensive traits including harmful algal toxin production in harmful algae. A group of polar lipids, copepodamides, have been identified as cueing compounds, and suggested to act as general alarm cues in the ocean. While a variety of defensive traits are demonstrably induced by copepodamides, only a limited number of taxa have been experimentally evaluated. Here we expose three previously untested harmful dinoflagellates to copepodamides and show that they too respond with increased toxin production, bioluminescence, or both. Our findings corroborate the role of copepodamides as general alarm cues in marine plankton. Moreover, the simultaneous up-regulation of both bioluminescence and toxicity shows that harmful algae can co-express defensive traits, which may have contributed to inconsistencies in experimental evaluations of costs and benefits of toxins and their role in harmful algal bloom formation.

This study adds to the growing literature on the indirect effects of grazers on community structure in the plankton and supports their suggested role in harmful algal bloom formation. We show that toxin production in two harmful algae taxa is under tight control from grazer cues, which provides new research opportunities to improve our understanding of harmful algal bloom formation and harmful algal bloom forecasting – topics of interest to the L&O readership.

Author contributions

Paula Gonzalo-Valmala: Conceptualization; Data curation; Formal analysis; Investigation; Methodology; Validation; Visualization; Writing – Original Draft Preparation; Writing – Review and Editing.

Milad Pourdanandeh: Data curation; Formal analysis; Methodology; Validation; Visualization; Writing – Original Draft Preparation; Writing – Review and Editing; Supervision.

Sandra Lage: Formal analysis; Funding acquisition; Investigation; Writing – Review and Editing.

Erik Selander: Conceptualization; Formal analysis; Funding acquisition; Methodology; Validation; Project Administration; Resources; Validation; Writing – Original Draft Preparation; Writing – Review and Editing; Supervision.

Abstract

Marine copepods are the most abundant type of multicellular zooplankton in the global oceans. They imprint their surrounding waters with a unique bouquet of polar lipids; copepodamides. Copepodamides are recognized by prey organisms, who respond by inducing defensive traits including bioluminescence, toxin production, colony size plasticity and structural modifications. Copepodamides are suggested to act as general alarm-cues, but only a limited number of species have been experimentally exposed to copepodamides to date. Here, we quantify bioluminescence and toxin content in response to increasing concentrations of copepodamides in three additional species of marine dinoflagellates: *Alexandrium catenella*, *Protoceratium reticulatum*, and *Gymnodinium catenatum*. All three species up-regulated their defensive traits in response to copepodamide exposure. Neither bioluminescence nor toxin production was associated with

measurable costs in terms of reduced growth rates. The results corroborate the role of copepodamides as general alarm-cues in marine phytoplankton. Moreover, the expression of simultaneous defensive traits in *A. catenella* may confound studies addressing the costs and benefits of these co-varying traits.

Introduction

Phytoplankton are the principal primary producers in the marine food webs (Field et al., 1998; Frederiksen et al., 2006; Pershing et al., 2015). Phytoplankton production is largely consumed by zooplankton, which play a multifaceted role in regulating processes such as the nutrient cycling (Sailley et al., 2015; Meunier et al., 2016), transfer of energy to higher trophic levels (Turner, 2004; Heneghan et al., 2016), and community composition of microalgae (Bergquist et al., 1985). Copepods average 90% of the metazooplankton biomass (Froneman, 2001; Pane et al., 2004) and are key grazers on microphytoplankton. Copepods release a bouquet of chemical compounds that induce defensive traits in prey organisms (Selander et al., 2006, 2019). The active substance was identified in 2015 as a group of polar lipids named copepodamides (Selander et al., 2015). Copepodamides divide into two groups separated only by the presence of a methyl or methylene group in position C3 (Selander et al., 2015). In addition, copepodamides have a variable fatty acid moiety and to date 41 unique copepodamide structures have been described (Selander et al., 2015; Grebner et al., 2019; Arnoldt et al., 2024). All calanoid and cyclopoids tested so far, from both limnic and marine environments, contain copepodamides (Arnoldt et al., 2024). Despite their omnipresence in copepods, the physiological role of copepodamides in copepods is still unknown. Similar compounds have, however, been suggested to function as emulsifiers facilitating lipid uptake (Grebner et al., 2019).

Phytoplankton prey organisms sense low (femto- to picomolar) naturally occurring concentrations of copepodamides and response by lunching a variety of defensive traits. The responding organisms include diverse representatives of diatoms, dinoflagellates, ciliates, and dicthyocophyceae (Selander et al., 2015, 2019; Arias et al., 2021; Rigby et al., 2024). The induced defense strategies include bioluminescence (Lindström et al., 2017; Prevett et al., 2019), amnesic shellfish toxin (AST) production (Selander et al., 2015; Olesen et al., 2022), paralytic shellfish toxin (PST) production (Selander et al., 2015; Ryderheim et al., 2021), colony size plasticity (Bergkvist et al., 2012; Selander et al., 2012) and silification in diatoms (Grønning & Kiørboe, 2020). In addition, copepodamides trigger changes in community composition in eukaryote- and bacterioplankton in a similar way that actual grazing from copepods do, suggesting that the presence of copepodamides alone can drive trait mediated cascading effects (Rigby et al., 2024).

Copepodamide-induced production of harmful algal toxins has been suggested to contribute to harmful algal bloom (HAB) formation. In addition to the induced increase in toxin production, copepods tend to selectively reject cells with up-regulated defense mechanisms (Esaias & Curl, 1972; Huntley et al., 1986; Prevett et al., 2019; Olesen et al., 2022), thereby increasing their relative abundance in the phytoplankton community (Cusick & Widder, 2020). This grazer-induced competitive edge could partly explain the success of defended dinoflagellates despite their typically slow growth rates and poor abilities to compete for nutrients (Banse, 1982; Smayda, 1997; Litchman et al., 2007). Ecological models of optimal defense assume that induction of defensive traits must entail some sort of cost for the cells, but one that is smaller than the benefit of the defense (McKey, 1974; McKey et al., 1979; Rhoades, 1979). However, the literature on the ecological costs associated with defensive traits in phytoplankton is highly

inconsistent and includes both negative costs (faster growth in more defended cells), and direct costs manifesting in lower growth rates (Ryderheim et al., 2021).

While copepodamides appear to be general defense inducers in phytoplankton, only a limited subset of phytoplankton have been experimentally exposed to copepodamides, and they also include organisms that do not show a marked response to copepodamides, e.g. the diarrhetic shellfish toxin producer genus *Dinophysis* sp. (Pourdanandeh et al., 2025). To evaluate the generality of the response it is necessary to increase the coverage of responding species.

Among the common HAB-forming dinoflagellates that have not yet to been experimentally exposed to copepodamides we find *Alexandrium catenella*, *Protoceratium reticulatum*, and *Gymnodinium catenatum*. *A. catenella* and *G. catenatum* produce paralytic shellfish toxins in response to copepod presence. It is, however, not known if this response is mediated by copepodamides or other copepod derived compounds (Selander et al., 2016; Griffin et al., 2019; Park et al., 2024). Both *A. catenella* and *P. reticulatum* are bioluminescent, a trait that correlates to efficient grazer deterrence (Prevett et al., 2019). The grazer deterrent effect of bioluminescence is not fully understood. Three competing hypotheses have been put forward. The first suggests that bioluminescence triggers a startling response in the copepod that allows the dinoflagellate to escape (Esaias & Curl, 1972), the second that bioluminescence serves as a "burglar alarm", where the emitted light attracts the grazers own predators (Burkenroad, 1943), and the third that bioluminescence is an aposematic warning, signaling its toxicity to the predator (Hanley & Widder, 2017). From this perspective it is notable that at least 12 common bioluminescent bloom-forming species in the genera *Alexandrium, Gonyaulax, Lingulaulax, Protoceratium* and *Pyrocistis* are known to be toxic (Cusick & Widder, 2020). For example, certain strains of *P. reticulatum* produce yessotoxins. This co-occurrence of bioluminescence and

toxicity raises the question of whether these defensive traits are regulated independently or in concert when exposed to copepodamides.

Here we exposed the three dinoflagellates *Alexandrium catenella*, *Protoceratium reticulatum*, and *Gymnodinium catenatum* to copepodamides and hypothesized that copepodamides would induce toxin production in *G. catenatum*, bioluminescence in *P. reticulatum*, and both toxin production and bioluminescence in *A. catenella*. We further predicted that grazer-induced stimulation of toxin and bioluminescence would be accompanied by a direct allocation cost that would manifest as reduced growth rates, with the greatest cost incurred by species that simultaneously up-regulate both phycotoxins and bioluminescent capacity.

Materials and Methods

Cell cultures

Gymnodinium catenatum (IO13-27-02), was isolated from Cascais, Portugal, September 2018. *Protoceratium reticulatum* (109), and *Alexandrium catenella* (130), were obtained from the Gothenburg University marine algae collection (GUMACC). *Gymnodinium catenatum* was grown in a dark:light cycle of 12:12 h and at ~19ºC. *Alexandrium catenella* and *Protoceratium reticulatum* in a reversed dark:light cycle of 10:14h at ~16ºC to allow daytime sampling of dark adapted cultures as bioluminescence is largely absent during the light phase. All three were cultured under a photon flux of 135 µmol m^2s^{-1}. The cultures were re-inoculated (~1:2, inoculum:media) every 7-14 days with fresh L1 medium (Guillard & Hargraves, 1993) with a salinity of 26 g/kg. Experiment cultures with the appropriate volume were prepared the week before the experiment and kept under the above-mentioned conditions to ascertain exponentially

146 growing starting materials. All handling of *P. reticulatum* and *A. catenella* was performed during
147 the light phase to avoid exhausting the bioluminescence (Valiadi & Iglesias-Rodriguez, 2013).

148 **Dose-response experiments**

149 *Experimental set-up*

150 Dose response experiments were carried out in glass tubes (12 x 75 mm) coated with 1-2 µL
151 copepodamides (CA) form *Calanus finmarchicus* dissolved in methanol (Selander et al., 2015).
152 The composition of the copepodamide extracts used can be seen in the Supporting Information
153 Table S1. *Alexandrium catenella* and *Protoceratium reticulatum* were exposed to 0, 0.5, 1 and 5
154 nM (n = 4 replicates) and *Gymnodinium catenatum* to 0, 0.1, 0.2, 0.5 and 1 nM of
155 copepodamides (n = 5 replicates). Lower copepodamide concentrations were used for *G.*
156 *catenatum* according to previous experiment results (data not shown). Controls received the
157 same amount of methanol without copepodamides. The solvent was evaporated in the fume hood
158 and 1-2 mL of cell cultures were added (1mL for bioluminescent experiments and 2 mL for toxin
159 induction experiments). Copepodamides rapidly degrade in sea water (Selander et al., 2019), so
160 cell cultures were transferred to freshly coated glass tubes every 48 hours to maintain exposure.

161 *Bioluminescence measurements*

162 Bioluminescence was measured on days 0, 1, 3, and 5 using a Berthold FB12 luminometer
163 (Titrek-Berthold, Berthold Detection Systems GmbH, Pforzheim, Germany). Measurements
164 were taken 3 hours into the dark phase, when cells are dark adapted and bioluminescent (Biggley
165 et al., 1969). Each tube was carefully transferred to the luminometer, and the total
166 bioluminescent capacity was triggered by the addition of 1:1 volumes of 1M acetic acid (aq). A
167 well-mixed aliquot (100-200 µL) of each sample was added onto a 96-well plate, fixed with

Lugol's solution and counted manually at 10x magnification (Olympus CK40) or through imaging (COE-200-M-USB-080-IR-C Opto Engineering Camera, Olympus CKX41 fitted to the camera port of the stereomicroscope) and automated cell counting with Fiji ImageJ (Schindelin et al., 2012).

Toxin measurements

G. catenatum and *A. catenella* were harvested after 0 (start values), 4 and 8 days by centrifuging the samples for 10 minutes at 2000 RCF at 4º C for *G. catenatum* (Allegra X-30R Centrifuge, Beckman Coulter) and 13 000 RPM at room temperature for *A. catenatum* (Heraecus Biofuge Pico). The supernatant was gently removed, and the pellets stored frozen until analysis (-20ºC). Pellets in *A. catenella* were fragile and the cells lost when removing the supernatant were manually counted (Olympus CK40, 10x magnification) and accounted for when calculating cell specific toxicity. Samples were freeze-dried (Heto LyoLab 3000 lyophilizer) before extraction through 3 consecutive freeze-thaw cycles in 300 µL 0.05 M Acetic acid. The extracts were centrifuged as above, filtered through a low volume glass fiber filter (GF/F, Whatman) and transferred to HPLC vials. The toxin analysis of regulated PSTs was performed through a Liquid Chromatography-High Resolution Mass Spectrometer (LC-HRMS) using commercially available standards as described in Lage et al. (2022).

Calculations, statistical analysis and visualization

Bioluminescence

Total bioluminescence capacity was extracted by integrating the luminometer readout from just before the addition of acetic acid until the light intensity returned to background levels. Bioluminescence per cell was calculated by dividing the light measurements by the number of

cells in each tube. The data was expressed as percentage increases relative to the controls and fitted to the Michaelis-Menten equation as:

$$Response\ variable\ increase = \frac{Vmax*[copepodamides]}{Km+[copepodamides]} \quad \text{(Eq. 1)}$$

where Vmax corresponds to the maximum response variable (RV, bioluminescence or toxins) increases and Km is the concentration of copepodamides needed to reach half of the maximum RV induction, together characterizing both the reaction norm and the relevant concentration needed to trigger the response.

Growth rates and net toxin/bioluminescence production

Specific growth rates were calculated as:

$$\mu = \frac{(\ln N_t - \ln \langle N_{t-1} \rangle)}{t_t - t_{t-1}} \quad \text{(Eq. 2)}$$

where N_t and N_{t-1} are the cell concentrations (cell per mL) at time *t* and the previous sampling occasion *(t-1).*

The production rate per cell and day, *R*, was calculated for both bioluminescence (Rbiolum) and toxins (Rtox) as:

$$R = \frac{(BT_t - BT_{t-1})}{(\bar{N})(\Delta t)} \quad \text{(Eq. 3)}$$

Where BT is the bioluminescence or toxin content per mL sample at two time points, $\bar{N}$ is the average concentration of cells, and Δt is the elapsed time (Anderson et al., 1990). $\bar{N}$ is calculated as:

$$\bar{N} = \frac{N_t - N_{t-1}}{lnN_t - lnN_{t-1}} \quad \text{(Eq. 4)}$$

Statistical analyses

Bioluminescence and toxin induction experiments in response to CA treatments were analyzed using *a priori* planned contrast variance analysis (Ruxton & Beauchamp, 2008; Quinn & Keough, 2023a) comparing treatment groups against controls. These were conducted separately for each sampling day (days 1, 3, and 5 for bioluminescence, days 4 and 8 for toxins) after confirming that there were no interaction effects between sampling day and treatment using two-factor ANOVAs. The assumption of equal variance of errors (homoscedasticity) for all linear models were assessed using residuals-versus-fitted plots. Data was Log_{10}-transformed if deviations from the expected null relationship were observed. The assumption of heteroscedasticity and normality were not formally tested, as ANOVAs in balanced experimental designs are generally robust to violations of their assumptions (Glass et al., 1972; Harwell et al., 1992; Lix et al., 1996), especially to non-normality (Gelman & Hill, 2006; Quinn & Keough, 2023b). The 5 nM treatment in the *A. catenella* experiment was excluded from the final statistical analysis, as its induction effects were comparable to those of the 0.5 and 1 nM treatment groups across both sampling days but also contributed to severely unequal error variances (Supporting Information Fig. S1). Potential allocation costs of bioluminescence or toxin induction were assessed visually and with correlation analyses. The level of significance was set to $\alpha = 0.05$ for all statistical tests.

Unless stated otherwise, summary statistics are presented as mean ± 95% CI, mean (95% CI range), or (mean, 95% CI). Effect sizes were calculated as log response ratios (LRR; Hedges et al., 1999) and reported as mean percentage increases with 95% CI ranges, e.g., as mean (lower–upper CI) or as ranges of mean percentage increases for multiple groups.

All statistical analyses and visualizations were performed in R v.4.4.1 (R Core team, 2024) using RStudio v.2024.4.1.748 (Posit team) and packages: *readxl* (Wickham & Bryan, 2023), *car* (Fox & Weisberg, 2019), *drc* (Ritz et al., 2015), *DescTools* (Signorell, 2025), *afex* (Singmann et al., 2024), *broom* (Robinson et al., 2024), *tidyverse* (Wickham et al., 2019), *Rmisc* (Hope, 2022), *ggtext* (Wilke & Wiernik, 2022), *ggpubr* (Kassambara, 2023), kableExtra (Zhu, 2024), *patchwork* (Pedersen, 2024), *cowplot* (Wilke, 2024), *ggplot2* (Wickham, 2016), *wesanderson* (Ram & Wickham, 2023), *grid* (R Core Team, 2024), *ggimage* (Yu, 2023).

The analysis code with all output, and the datasets it uses to perform all statistical analyses and produce visualizations are openly accessible at https://doi.org/10.5281/zenodo.14883074.

Results

Bioluminescence

The two bioluminescent dinoflagellates, *Protoceratium reticulatum* and *Alexandrium catenella* both responded to copepodamides with increased bioluminescent capacity (Fig. 1a-b). The response developed over time and doubled from 32-37% on day 1 to 53-83 % after 5 days of exposure relative to controls (Table 1.). Half saturation values (Km) were generally lower for *A. catenella* (mean 0.17 nM) than *P. reticulatum* (mean 0.51 nM, Table 1), indicating that *A. catenella* is more sensitive to copepodamides than *P. reticulatum*. Growth rates averaged 0.14 ± 0.06 day^{-1} and 0.11 ± 0.09 day^{-1} (mean ± SD) for *A. catenella* (Fig. 1c) and *P. reticulatum* (Fig. 1d) respectively. Net bioluminescence production rate (RLU $cell^{-1}$ day^{-1}) was not significantly correlated with growth rate for *A. catenella* ($r = -0.01$, $p = 0.9$, Fig. 1e) or *P. reticulatum* ($r = -0.17$, $p = 0.2$, Fig. 1f).

Table 1. Constants from the Michaelis-Menten curve fits to copepodamide induced bioluminescence increase in *A. catenella* and *P. reticulatum*. The half saturation constant (Km) shows the concentration needed to trigger half the maximum bioluminescence increase (Vmax) relative to control.

Sp.	**Day**	**Km (nM)**	**Vmax (%)**
A. catenella	3	0.11	50.57
	5	0.22	61.33
P. reticulatum	1	0.51	42.29
	3	0.65	75.28
	5	0.37	83.32

Table 2. Summary statistics of copepodamide-induced bioluminescence experiments for *Protoceratium reticulatum* and *Alexandrium catenella.* CA (nM) denotes nominal copepodamide concentration in the treatment groups, effect size of mean bioluminescence increase compared to controls and its 95% CI are derived from the log response ratio. Treatment groups significantly different from their controls ($p < 0.05$) in a planned-contrast variance analysis are denoted in bold.

Species	Day	CA (nM)	Effect size (%)	95 CI (%)	p - value
P. reticulatum	1	0.5	17.9	-13.5 – 60.8	0.136
		1	**31.5**	-4.2 – 80.7	**0.015**
		5	**37.2**	-4.9 – 98.3	**0.006**
	3	0.5	**40.8**	8.4 – 82.7	**0.001**
		1	**36**	8.4 – 70.6	**0.003**
		5	**69**	34.7 – 112	**< 0.001**
	5	0.5	59.8	-25.0 – 241	0.092
		1	44	-32.8 – 208.6	0.203
		5	**83.3**	-27.4 – 363.25	**0.025**
A. catenella	1	0.5	**36.6**	9.0 – 71.1	**0.001**
		1	**35**	9.8 – 66.0	**0.002**
		5	**36**	2.6 – 80.3	**0.001**
	3	0.5	30.3	-8.6 – 86.0	0.055
		1	**65.3**	-4.3 – 185.5	**0.002**
		5	**40.1**	4.7 – 87.5	**0.018**
	5	0.5	40.1	-19.3 – 143.37	0.126
		1	**53.4**	-20.1 – 195.0	**0.049**
		5	**57.3**	-9.69 – 174.0	**0.037**

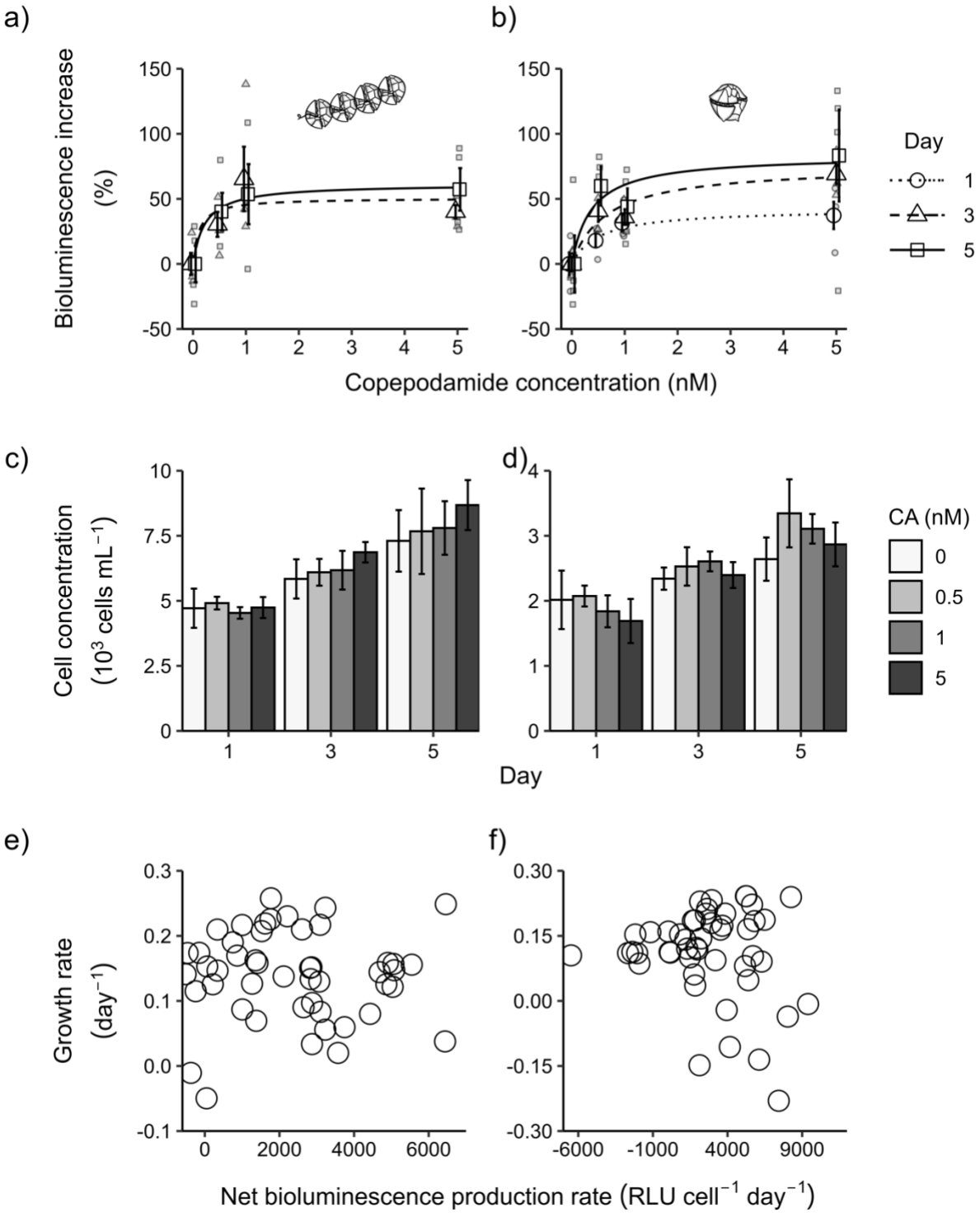

Fig 1. (a-b): Michaelis-Menten curve fit for dose-response experiment as percentage increase in bioluminescence relative to controls in response to increasing copepodamide concentrations for (**a**)

Alexandrium catenella and, (**b**) *Protoceratium reticulatum* after 1, 3 and 5 days of copepodamide exposure. Small filled geometric shapes are individual replicate values, large hollow shapes are mean values of n = 4 replicates, and error bars denote 95% confidence intervals. (**c-d)**: Cell concentrations for each copepodamide treatment after 1, 3 and 5 days for (**c**) *A. catenella* and (**d**) *P. reticulatum*. Bars are mean values of n = 4 replicates and the error bars denote 95% confidence intervals. **(e-f)**: Scatter plots of growth rates and net bioluminescence production rates for (**e**) *A. catenella* and (**f**) *P. reticulatum*.

Paralytic shellfish toxins (PSTs)

The toxin profile of *A. catenella* was dominated by neosaxitoxins (Neo), GTX4 and saxitoxins (STX) and trace amounts of decarbamoyl derivatives (dcSTX, dcGTX4, dcGTX3) and N-sulfocarbamoyl toxin C2 (Fig. 2b), whereas *Gymnodinium catenatum* predominantly produced the C2 congener with trace amounts of GTX3, Neo, STX, dcSTX, C4 and GTX6 (Fig. 2a). *G. catenatum* toxins significantly increased by the first sampling day, peaking on day four with up to ten-fold higher cell specific toxin content (Table 3, Fig. 2a) than controls. On day 8, the difference was less pronounced, with a significant increase of 259% (22-959) compared to controls in the 1 nM treatment only ($p = 0.011$, Fig. 2a). *A. catenella* showed a similar, although marginally non-significant, trend with increasing toxin content in copepodamide exposed cultures (Fig. 2b). Cell specific toxin content averaged 63% higher (p 0.12-0.16) than controls after four days and 103-104 % more after eight days ($p = 0.1$ and 0.05 for 0.5 and 1 nM respectively, Fig. 2b).

Growth rates averaged 0.09 ± 0.06 day^{-1} and 0.12 ± 0.05 day^{-1} (mean ± SD) for *A. catenella* (Fig. 2c) and *G. catenatum* (Fig. 2d) respectively. Net toxin production rate (fmol cell^{-1} day^{-1}) was not significantly correlated with the growth rate of *A. catenella* ($r = -0.04$, $p = 0.8$, Fig. 2f) or *G. catenatum* ($r = 0.06$, $p = 0.7$, Fig. 2f).

Table 3. Summary statistics of the copepodamide-induced toxin experiments for *Alexandrium catenella* and *Gymnodinium catenatum.* CA (nM) denotes nominal copepodamide concentration in the treatment groups, effect size of mean toxin increase compared to controls and its 95% CI are derived from the log response ratio. Treatment groups significantly different from their controls ($p < 0.05$) in a planned-contrast variance analysis are denoted in bold.

Species	Day	CA (nM)	Effect size (%)	95 CI (%)	p - value
A. catenella	4	0.5	62	-39.7 – 335.6	0.163
		1	64.1	-42.1 – 365.5	0.124
	8	0.5	104.2	58.3 – 163.4	0.096
		1	103.2	22.8 – 236.1	0.053
G. catenatum	4	0.1	**754.3**	175.1 – 2552.3	**< 0.001**
		0.2	**792.3**	202.4 – 2532.5	**0.001**
		0.5	**1099**	270.2 – 3783.5	**< 0.001**
		1	**850.4**	206.9 – 2843-2	**0.0001**
	8	0.1	72	-46.0 – 448.5	0.3
		0.2	64.7	-60.9 – 595.0	0.65
		0.5	159.1	-17.8 – 716.0	0.077
		1	**258.8**	21.6 – 958.7	**0.011**

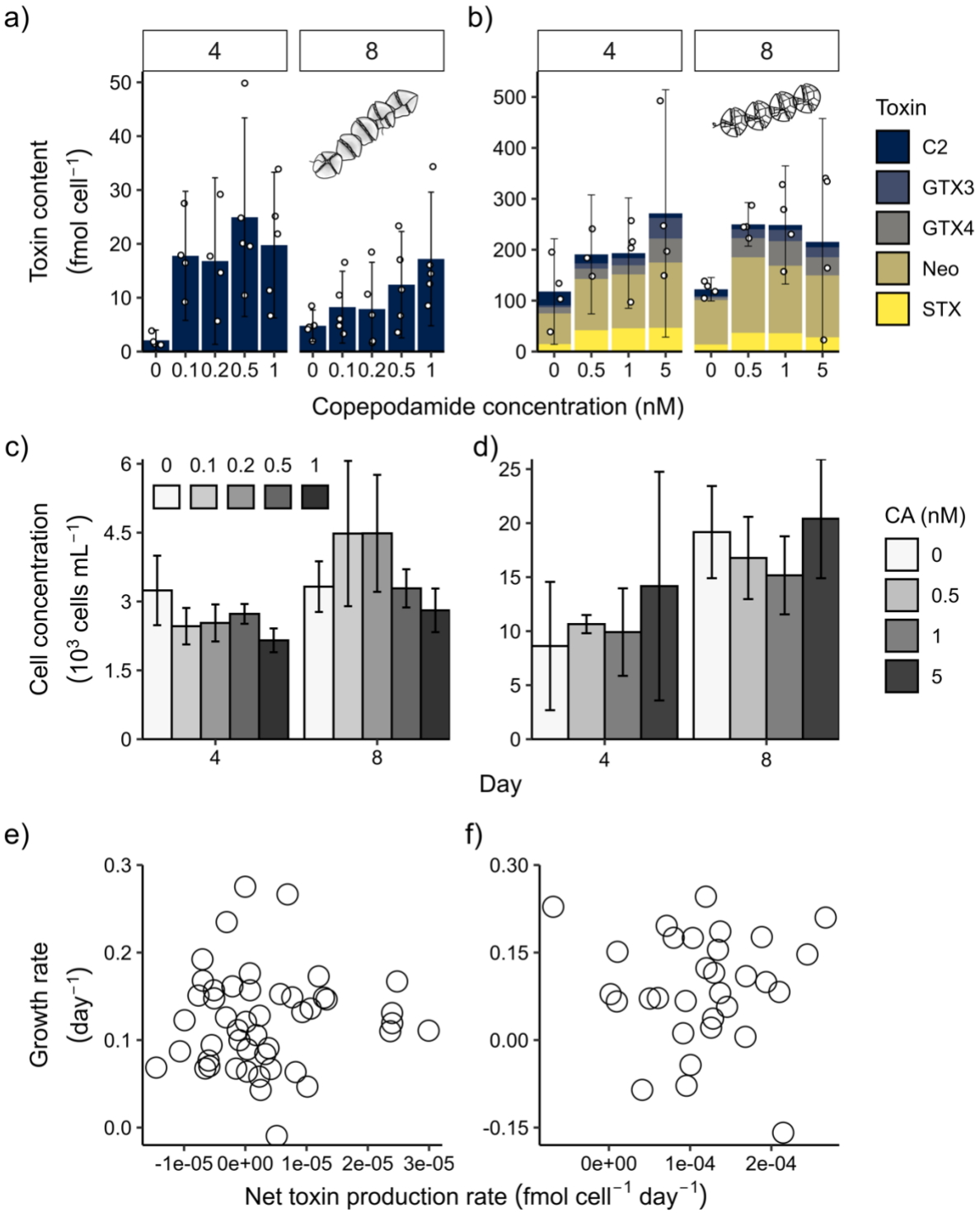

304

305 **Fig. 2 (a-b):** Paralytic shellfish toxin (PST) profiles (C2: N-Sulfocarbamoyl-gonyautoxin-2, GTX3:

306 Gonyautoxin-3, GTX4: Gonyautoxin-4, Neo: Neosaxitoxin, STX: Saxitoxin) for (**a**) *Gymnodinium*

catenatum and (**b**) *Alexandrium catenella* across copepodamide treatments and days (4-8). Colored bars are means of each toxin congeners based on n = 4 replicates for *A. catenella* and n = 5 replicates for *G. catenatum*, and error bars denote 95% confidence intervals of pooled toxins. An outlier replicate in CA treatment 0.5 nM on day 8 is not visible in **b**. **(c-d):** Cell concentrations for each copepodamide treatment after 4 and 8 days for (**c**) *G. catenatum* and (**d**) *A. catenella*. Bars are mean values of n = 4 and 5 replicates, respectively, and error bars denote 95% confidence intervals. **(e-f):** Scatter plots of growth rates and net toxin production rates for (**e**) *G. catenatum* and (**f**) *A. catenella.*

Discussion

All the three species of dinoflagellates in this study responded to copepodamides by expressing a more defended phenotype, corroborating the role of copepodamides as a general defense inducer in phytoplankton organisms. *Protoceratium reticulatum* increased its bioluminescent intensity, *Gymnodinium catenatum* enhanced its paralytic shellfish toxin (PST) content and *Alexandrium catenella* up-regulated bioluminescence and showed a strong trend towards upregulating PSTs ($p = 0.053$-0.096). The effective copepodamide concentrations are a result of slow desorption from the coated culture vessel and the degradation of copepodamides in the culture media over time. The effective CA concentrations in a similar experimental set-up were measured and averaged to approximately 1% of the nominal concentrations over 48 h after exposure (Selander et al., 2019; Supplementary Material). The half saturation constants (Km) for the bioluminescence induction experiments varied between nominal CA concentrations of 0.11 – 0.22 nM in *A. catenella* and 0.37 – 0.65 nM in *P. reticulatum* (Table 1). This corresponds to average effective copepodamide concentrations of 1.1 – 2.2 pM and 3.7 – 6.5 pM, respectively, which is on par with the natural concentrations of copepodamides found in nature (40 fM - 2 pM) (Selander et al., 2019). In the ocean, in situ concentrations of these grazer cues

experience fluctuations that follow copepod biomass and is thus provide a reliable proxy of the copepod densities for the responding algae. Moreover, copepods can sometimes reach densities of hundreds per liter (Hamner & Carleton, 1979; Ambler et al., 1991) and a single copepod can exude up to 120 pmol a day (Selander et al., 2015), indicating that even the higher copepodamide concentrations of our treatment could likely be found within a natural occurring range and be ecologically relevant. The copepodamides used in this study were purified from freeze-dried *Calanus finmarchicus* and contains a lower proportion of dihydro-copepodamides (methylene-containing copepodamides) compared to natural samples from both limnic and temperate marine copepods (Arnoldt et al., 2024). Given that dihydro-copepodamides may be more potent toxin inducers that their methyl-containing counterparts (Selander et al., 2015), our observed effects may be conservative compared to the exposure to the copepodamide profiles found in the natural environment of the responders.

Trade-offs in phytoplankton defenses manifest as reductions in grazer-induced mortality rates associated with lower growth rates (Pančić & Kiørboe, 2018). Theory predicts that the benefit associated with an inducible defense mechanism should incur a cost (McKey, 1974; McKey et al., 1979; Rhoades, 1979), otherwise, all phytoplankton species would evolve to develop an equal state of protection (Stamp, 2003; Pančić & Kiørboe, 2018). Quantitative understanding of this trade-of is necessary to predict the outcome of this predator-prey relationship, yet this inquiry is rarely covered and results are inconsistent (Pančić & Kiørboe, 2018). *A. catenella* has, based on indirect correlation with *cyc* gene (a genetic growth marker), been suggested to grow slower when toxin production increased in response to copepod grazers (Park et al., 2023). Likewise, growth rates decreased with increased grazer-induced domoic acid production in *Pseudo-nitzschia* sp (Lundholm et al., 2018). In contrast, copepod-mediated toxin induction had

353 no effect on the growth of *Alexandrium tamarense* (Selander et al., 2011), and resulted in
354 increased growth rate for *Alexandrium minutum* (Ryderheim et al., 2021). None of the grazer-
355 induced defenses observed here correlated with changes in growth rates (Fig. 1e-f & Fig. 2e-f).
356 The conditions for these experiments, where cells were in constant exponential growth phase
357 with abundant access to nutrients, combined with the absence of resource competition with other
358 species, is arguably a poor mimic for the conditions found in the ocean (Bristow et al., 2017).
359 Under our near optimal conditions, compromising their growth for defenses might not be
360 required to maintain fitness. There was a weak trend towards lower growth rates in the most
361 bioluminescent species, *P. reticulatum*, which could indicate that bioluminescence may be costly
362 in this species. This is supported by the circadian regulation of bioluminescence capacity
363 observed in some dinoflagellates. Some species are known to daily degrade and re-synthesize the
364 scintillons and its bioluminescent machinery, exhibiting light only on the dark hours of the day
365 (Dunlap & Hastings, 1981), whereas bioluminescence is conserved in other species by relocating
366 scintillons within the cell during the light phases of the cycle (Colepicolo et al., 1993). Both
367 mechanisms are expected to incur energetic costs: the first through the daily transduction of
368 luciferin-related components (binding protein, enzymes, and substrate mRNA) and their
369 subsequent degradation (Hastings, 2013), and the latter through the maintenance and relocation
370 of the bioluminescent machinery within the cell (Valiadi & Iglesias-Rodriguez, 2013).
371 *A. catenella* appears to simultaneously increase bioluminescence and toxin production. This
372 is one of few examples of phytoplankton expressing multiple defenses in response to predator
373 cues. Selander et al. (2011) and Lindström et al. (2017) found that the same strain of
374 *Alexandrium tamarense* (no.3, GUMAC) induced both bioluminescence and changes in chain
375 length in response to copepod grazer cues. Similarly, Selander et al. (2012) observed chain

length shortening in concert with increased toxin production for two additional strains of *A. tamarense* (no.1 and no.9, GUMACC), suggesting that *A. tamarense* may be capable of simultaneously up-regulating three (or more, hitherto unknown) defensive traits in response to zooplankton cues. Multiple defense strategies may provide a more robust protection against grazers and may also fine-tune the composition of defensive traits to the composition of the grazing community (Smayda & Reynolds, 2003; Long et al., 2007). Moreover, the presence of multiple defense strategies within a single organism is an important factor to consider when resolving the costs and benefits of defensive traits. Cost-benefit analyses are typically performed on single traits and both costs and benefits may consequently be confounded by the simultaneous onset of additional, non-monitored traits. In Park et al. (2023) toxin production in *A. catenella* was associated with reduced growth rates through correlation with genetic growth markers. The authors suggest that this reflects an allocation cost associated with toxin production. Here, toxin induction was less pronounced than in their experiment and we saw no significant reduction in growth rate. The simultaneous onset of increased bioluminescence, however, suggests that the cost in Park and colleagues study may also encompass the cost of bioluminescence.

The community structure and composition of phytoplankton is regulated both by a bottom-up control of resource availability (Manzi Marinho & de Moraes Huszar, 2002; Moschonas et al., 2017; Burson et al., 2018) and via top-down grazing pressure from zooplankton (McCauley & Briand, 1979; Kenitz et al., 2017). Phytoplankton may consequently increase their fitness both through competition and by resisting predation. Dinoflagellates are generally poor competitors under nutrient limited conditions compared to e.g. diatoms and non-toxic flagellates (Riegman et al., 1996; Yamamoto & Tarutani, 1999). In contrast, they are overrepresented among the harmful algal bloom (HAB) producing taxa (Smayda, 2002). By adjusting their

defense level to the level of threat, phytoplankton can optimize their fitness. Prevett et al. (2019) illustrated how bioluminescent *Lingulaulax polyedra* (previously *Lingulodinium polyedra*) went from being the preferred prey of copepod *Acartia tonsa* to completely rejected when up-regulating bioluminescent capacity in response to copepod cues. Multiple studies have indicated this feeding preference of copepods towards non-bioluminescent cells versus bioluminescent ones (Esaias & Curl, 1972; White, 1979). Likewise, strong evidence supports the importance of defense traits for enabling large dinoflagellates to compete with smaller and faster growing phytoplankton (Guisande et al., 2002; Ryderheim et al., 2021).

In conclusion, this study adds three species to the list of phytoplanktonic species capable of sensing and reacting to copepodamides. With array of phylogenetically distant microalgae demonstrating the ability to detect these alarm cues (Selander et al., 2015; Lindström et al., 2017; Grebner et al., 2019; Olesen et al., 2022), our findings further support the convergent evolution of this predator recognition mechanisms. Moreover, induced bioluminescence and toxin production correlate to efficient deterrence of copepods grazers (Guisande et al., 2002; Prevett et al., 2019; Ryderheim et al., 2021) and hence may contribute to the success of the studied species. Grazing pressure is redirected to the non-defended organisms, benefiting the harmful taxa, and thus potentially contributing to the formation of HABs. Clarifying the complex dynamics underlying these predator-prey interactions is crucial for understanding the mechanistic drivers of HAB formation and their broader impacts on marine ecosystems.

Conflict of Interest

The authors declare no conflict of interest

Acknowledgements

We thank the two master students, Hope Stenvenson and Malin Frisell, who performed pilot studies for these experiments and Jenny Lindström valuable for input on design and light measurements. We thank Gerry Quinn and Jonathan N. Havenhand for inspiration and support regarding the statistical analyses, and we are also grateful to Professor Ana Amorim, MARE – Marine and Environmental Sciences Centre, and Department of Plant Biology, Lisbon University, Portugal for kindly providing the *Gymnodinium catenatum* (IO13-27-02) strain from the algae culture collection of the Lisbon University (ALISU).

This work was funded by the Swedish Research Council grant to Erik Selander (VR 2019-05238). Sandra Lage was supported by "la Caixa" Foundation (ID 100010434) through a Junior Leader Retaining Fellowship (LCF/BQ/PR23/11980049), and Portuguese national funds from FCT—Foundation for Science and Technology through projects UIDB/04326/2020, UIDP/04326/2020, and LA/P/0101/2020; the operational programs CRESC Algarve 2020 and COMPETE 2020 through project EMBRC.PT ALG-01-0145-FEDER-022121.

References

Ambler, J. W., Ferrari, F. D., & Fornshell, J. A. (1991). Population structure and swarm formation of the cyclopoid copepod Dioithona oculata near mangrove cays. *Journal of Plankton Research*, *13*(6), 1257–1272. https://doi.org/10.1093/plankt/13.6.1257

Anderson, D. M., Kulis, D. M., Sullivan, J. J., Hall, S., & Lee, C. (1990). Dynamics and physiology of saxitoxin production by the dinoflagellates Alexandrium spp. *Marine Biology*, *104*(3), 511–524. https://doi.org/10.1007/BF01314358

Arias, A., Selander, E., Saiz, E., & Calbet, A. (2021). Predator Chemical Cue Effects on the Diel Feeding Behaviour of Marine Protists. *Microbial Ecology*, *82*(2), 356–364. https://doi.org/10.1007/s00248-020-01665-9

Arnoldt, S., Pourdanandeh, M., Spikkeland, I., Andersson, M. X., & Selander, E. (2024). Mass spectroscopy reveals compositional differences in copepodamides from limnic and marine copepods. *Scientific Reports*, *14*(1), 3147. https://doi.org/10.1038/s41598-024-53247-1

Banse, K. (1982). Cell volumes, maximal growth rates of unicellular algae and ciliates, and the role of ciliates in the marine pelagial1,2. *Limnology and Oceanography*, *27*(6), 1059–1071. https://doi.org/10.4319/lo.1982.27.6.1059

Bergkvist, J., Thor, P., Jakobsen, H. H., Wängberg, S.-Å., & Selander, E. (2012). Grazer-induced chain length plasticity reduces grazing risk in a marine diatom. *Limnology and Oceanography*, *57*(1), 318–324. https://doi.org/10.4319/lo.2012.57.1.0318

Bergquist, A. M., Carpenter, S. R., & Latino, J. C. (1985). Shifts in phytoplankton size structure and community composition during grazing by contrasting zooplankton assemblages. *Limnology and Oceanography*, *30*(5), 1037–1045. https://doi.org/10.4319/lo.1985.30.5.1037

Biggley, W. H., Swift, E., Buchanan, R. J., & Seliger, H. H. (1969). Stimulable and Spontaneous Bioluminescence in the Marine Dinoflagellates, *Pyrodinium bahamense, Gonyaulax polyedra* , and *Pyrocystis lunula*. *The Journal of General Physiology*, *54*(1), 96–122. https://doi.org/10.1085/jgp.54.1.96

Bristow, L. A., Mohr, W., Ahmerkamp, S., & Kuypers, M. M. M. (2017). Nutrients that limit growth in the ocean. *Current Biology*, *27*(11), R474–R478. https://doi.org/10.1016/j.cub.2017.03.030

Burkenroad, M. D. (1943). A possible function of bioluminescence. *Journal of Marine Research*, *5*, 161–164.

Burson, A., Stomp, M., Greenwell, E., Grosse, J., & Huisman, J. (2018). Competition for nutrients and light: testing advances in resource competition with a natural phytoplankton community. *Ecology*, *99*(5), 1108–1118. https://doi.org/10.1002/ecy.2187

Colepicolo, P., Roenneberg, T., Morse, D., Taylor, W. R., & Hastings, J. W. (1993). Circadian regulation of bioluminescence in the dinoflagellate *Pyrocystis lunula*. *Journal of Phycology*, *29*(2), 173–179. https://doi.org/10.1111/j.0022-3646.1993.00173.x

Cusick, K. D., & Widder, E. A. (2020). Bioluminescence and toxicity as driving factors in harmful algal blooms: Ecological functions and genetic variability. *Harmful Algae*, *98*, 101850. https://doi.org/10.1016/j.hal.2020.101850

Dunlap, J. C., & Hastings, J. W. (1981). The biological clock in Gonyaulax controls luciferase activity by regulating turnover. *Journal of Biological Chemistry*, *256*(20), 10509–10518. https://doi.org/10.1016/S0021-9258(19)68651-5

Esaias, W. E., & Curl, H. C. (1972). Effect of dinoflagellate bioluminescence on copepod ingestion rates. *Limnology and Oceanography*, *17*(6), 901–906. https://doi.org/10.4319/lo.1972.17.6.0901

Field, C. B., Behrenfeld, M. J., Randerson, J. T., & Falkowski, P. (1998). Primary Production of the Biosphere: Integrating Terrestrial and Oceanic Components. *Science*, *281*(5374), 237–240. https://doi.org/10.1126/science.281.5374.237

Fox, J., & Weisberg, S. (2019). *An R Companion to Applied Regression*. Sage. https://www.john-fox.ca/Companion/

Frederiksen, M., Edwards, M., Richardson, A. J., Halliday, N. C., & Wanless, S. (2006). From plankton to top predators: bottom-up control of a marine food web across four trophic levels. *Journal of Animal Ecology*, *75*(6), 1259–1268. https://doi.org/10.1111/j.1365-2656.2006.01148.x

Froneman, P. W. (2001). Seasonal Changes in Zooplankton Biomass and Grazing in a Temperate Estuary, South Africa. *Estuarine, Coastal and Shelf Science*, *52*(5), 543–553. https://doi.org/10.1006/ecss.2001.0776

Gelman, A., & Hill, J. (2006). Data Analysis Using Regression and Multilevel/Hierarchical Models. In *Analytical Methods for Social Research*. Cambridge University Press. https://doi.org/DOI: 10.1017/CBO9780511790942

Glass, G. V, Peckham, P. D., & Sanders, J. R. (1972). Consequences of Failure to Meet Assumptions Underlying the Fixed Effects Analyses of Variance and Covariance. *Review of Educational Research*, *42*(3), 237–288. https://doi.org/10.3102/00346543042003237

Grebner, W., Berglund, E. C., Berggren, F., Eklund, J., Harðadóttir, S., Andersson, M. X., & Selander, E. (2019). Induction of defensive traits in marine plankton—new copepodamide structures. *Limnology and Oceanography*, *64*(2), 820–831. https://doi.org/10.1002/lno.11077

Griffin, J. E., Park, G., & Dam, H. G. (2019). Relative importance of nitrogen sources, algal alarm cues and grazer exposure to toxin production of the marine dinoflagellate Alexandrium catenella. *Harmful Algae*, *84*, 181–187. https://doi.org/10.1016/j.hal.2019.04.006

Grønning, J., & Kiørboe, T. (2020). Diatom defence: Grazer induction and cost of shell-thickening. *Functional Ecology*, *34*(9), 1790–1801. https://doi.org/10.1111/1365-2435.13635

Guisande, C., Frangópulos, M., Maneiro, I., Vergara, A., & Riveiro, I. (2002). Ecological advantages of toxin production by the dinoflagellate Alexandrium minutum under phosphorus limitation. *Marine Ecology Progress Series*, *225*, 169–176. https://doi.org/10.3354/meps225169

Hamner, W. M., & Carleton, J. H. (1979). Copepod swarms: Attributes and role in coral reef ecosystems. *Limnology and Oceanography*, *24*(1), 1–14. https://doi.org/10.4319/lo.1979.24.1.0001

Hanley, K. A., & Widder, E. A. (2017). Bioluminescence in Dinoflagellates: Evidence that the Adaptive Value of Bioluminescence in Dinoflagellates is Concentration Dependent. *Photochemistry and Photobiology*, *93*(2), 519–530. https://doi.org/10.1111/php.12713

Harwell, M. R., Rubinstein, E. N., Hayes, W. S., & Olds, C. C. (1992). Summarizing Monte Carlo Results in Methodological Research: The One- and Two-Factor Fixed Effects ANOVA Cases. *Journal of Educational Statistics*, *17*(4), 315–339. https://doi.org/10.2307/1165127

Hastings, J. (2013). Circadian Rhythms in Dinoflagellates: What Is the Purpose of Synthesis and Destruction of Proteins? *Microorganisms*, *1*(1), 26–32. https://doi.org/10.3390/microorganisms1010026

Hedges, L. V, Gurevitch, J., & Curtis, P. S. (1999). THE META-ANALYSIS OF RESPONSE RATIOS IN EXPERIMENTAL ECOLOGY. *Ecology*, *80*(4), 1150–1156. https://doi.org/https://doi.org/10.1890/0012-9658(1999)080[1150:TMAORR]2.0.CO;2

533 Heneghan, R. F., Everett, J. D., Blanchard, J. L., & Richardson, A. J. (2016). Zooplankton Are
534 Not Fish: Improving Zooplankton Realism in Size-Spectrum Models Mediates Energy
535 Transfer in Food Webs. *Frontiers in Marine Science*, *3*.
536 https://doi.org/10.3389/fmars.2016.00201
537 Hope, R. M. (2022). *Rmisc: Ryan Miscellaneous*. https://CRAN.R-project.org/package=Rmisc
538 Huntley, M., Sykes, P., Rohan, S., & Marin, V. (1986). Chemically-mediated rejection of
539 dinoflagellate prey by the copepods *Calanus pacificus* and *Paracalanus parvus*:
540 mechanism, occurrence and significance. *Marine Ecology Progress Series*, *28*, 105–120.
541 https://doi.org/10.3354/meps028105
542 Kassambara, A. (2023). *ggpubr: "ggplot2" Based Publication Ready Plots*. https://CRAN.R-
543 project.org/package=ggpubr
544 Kenitz, K. M., Visser, A. W., Mariani, P., & Andersen, K. H. (2017). Seasonal succession in
545 zooplankton feeding traits reveals trophic trait coupling. *Limnology and Oceanography*,
546 *62*(3), 1184–1197. https://doi.org/10.1002/lno.10494
547 Lage, S., Costa, P. R., Canário, A. V. M., & Da Silva, J. P. (2022). LC-HRMS Profiling of
548 Paralytic Shellfish Toxins in Mytilus galloprovincialis after a Gymnodinium catenatum
549 Bloom. *Marine Drugs*, *20*(11), 680. https://doi.org/10.3390/md20110680
550 Lindström, J., Grebner, W., Rigby, K., & Selander, E. (2017). Effects of predator lipids on
551 dinoflagellate defence mechanisms - increased bioluminescence capacity. *Scientific*
552 *Reports*, *7*(1), 13104. https://doi.org/10.1038/s41598-017-13293-4
553 Litchman, E., Klausmeier, C. A., Schofield, O. M., & Falkowski, P. G. (2007). The role of
554 functional traits and trade-offs in structuring phytoplankton communities: scaling from

555 cellular to ecosystem level. *Ecology Letters*, *10*(12), 1170–1181.
556 https://doi.org/10.1111/j.1461-0248.2007.01117.x
557 Lix, L. M., Keselman, J. C., & Keselman, H. J. (1996). Consequences of Assumption Violations
558 Revisited: A Quantitative Review of Alternatives to the One-Way Analysis of Variance "F"
559 Test. *Review of Educational Research*, *66*(4), 579–619. https://doi.org/10.2307/1170654
560 Long, J. D., Smalley, G. W., Barsby, T., Anderson, J. T., & Hay, M. E. (2007). Chemical cues
561 induce consumer-specific defenses in a bloom-forming marine phytoplankton. *Proceedings*
562 *of the National Academy of Sciences*, *104*(25), 10512–10517.
563 https://doi.org/10.1073/pnas.0611600104
564 Lundholm, N., Krock, B., John, U., Skov, J., Cheng, J., Pančić, M., Wohlrab, S., Rigby, K.,
565 Nielsen, T. G., Selander, E., & Harðardóttir, S. (2018). Induction of domoic acid production
566 in diatoms—Types of grazers and diatoms are important. *Harmful Algae*, *79*, 64–73.
567 https://doi.org/10.1016/j.hal.2018.06.005
568 Manzi Marinho, M., & de Moraes Huszar, V. L. (2002). Nutrient availability and physical
569 conditions as controlling factors of phytoplankton composition and biomass in a tropical
570 reservoir (Southeastern Brazil). *Fundamental and Applied Limnology*, *153*(3), 443–468.
571 https://doi.org/10.1127/archiv-hydrobiol/153/2002/443
572 McCauley, E., & Briand, F. (1979). Zooplankton grazing and phytoplankton species richness:
573 Field tests of the predation hypothesis. *Limnology and Oceanography*, *24*(2), 243–252.
574 https://doi.org/10.4319/lo.1979.24.2.0243
575 McKey, D. (1974). Adaptive Patterns in Alkaloid Physiology. *The American Naturalist*,
576 *108*(961), 305–320. https://doi.org/10.1086/282909

McKey, D., Rosenthal, G. A., & Janzen, D. H. (1979). The distribution of secondary compounds within plants. In *Herbivores: Their interaction with secondary plant metabolites. Academic press* (pp. 55–134).

Meunier, C. L., Boersma, M., Wiltshire, K. H., & Malzahn, A. M. (2016). Zooplankton eat what they need: copepod selective feeding and potential consequences for marine systems. *Oikos*, *125*(1), 50–58. https://doi.org/10.1111/oik.02072

Moschonas, G., Gowen, R. J., Paterson, R. F., Mitchell, E., Stewart, B. M., McNeill, S., Glibert, P. M., & Davidson, K. (2017). Nitrogen dynamics and phytoplankton community structure: the role of organic nutrients. *Biogeochemistry*, *134*(1–2), 125–145. https://doi.org/10.1007/s10533-017-0351-8

Olesen, A. J., Ryderheim, F., Krock, B., Lundholm, N., & Kiørboe, T. (2022). Costs and benefits of predator-induced defence in a toxic diatom. *Proceedings of the Royal Society B: Biological Sciences*, *289*(1972). https://doi.org/10.1098/rspb.2021.2735

Pančić, M., & Kiørboe, T. (2018). Phytoplankton defence mechanisms: traits and trade-offs. *Biological Reviews*, *93*(2), 1269–1303. https://doi.org/10.1111/brv.12395

Pane, L., Feletti, M., Fancomacaro, B., & Mariottini, G. L. (2004). Summer coastal zooplankton biomass and copepod community structure near the Italian Terra Nova Base (Terra Nova Bay, Ross Sea, Antarctica). *Journal of Plankton Research*, *26*(12), 1479–1488. https://doi.org/10.1093/plankt/fbh135

Park, G., Norton, L., Avery, D., & Dam, H. G. (2023). Grazers modify the dinoflagellate relationship between toxin production and cell growth. *Harmful Algae*, *126*, 102439. https://doi.org/10.1016/j.hal.2023.102439

Park, J., Choi D., Kim, N., Hyun, M., Kim, Y., Noh, J., Rho, J., Park, B., Hong, S., Kim, S., Kim, M., Han, J., Han, Y., Lee, Y. (2024). Effects of Zooplankton Extracts on the Production of Paralytic Shellfish Toxins by Gymnodinium catenatum and Alexandrium pacificum. Ocean Science Journal, 59(4). doi:10.1007/s12601-024-00178-7

Pedersen, T. L. (2024). *patchwork: The Composer of Plots*. https://patchwork.data-imaginist.com

Pershing, A. J., Mills, K. E., Record, N. R., Stamieszkin, K., Wurtzell, K. V., Byron, C. J., Fitzpatrick, D., Golet, W. J., & Koob, E. (2015). Evaluating trophic cascades as drivers of regime shifts in different ocean ecosystems. *Philosophical Transactions of the Royal Society B: Biological Sciences*, *370*(1659), 20130265. https://doi.org/10.1098/rstb.2013.0265

Pourdanandeh, M., Séchet, V., Carpentier, L., Réveillon, D., Hervé, F., Hubert, C., Hess, P., & Selander, E. (2025). Effects of copepod chemical cues on intra- and extracellular toxins in two species of Dinophysis. *Harmful Algae*, *142*, 102793. https://doi.org/10.1016/j.hal.2024.102793

Prevett, A., Lindström, J., Xu, J., Karlson, B., & Selander, E. (2019). Grazer-induced bioluminescence gives dinoflagellates a competitive edge. *Current Biology*, *29*(12), R564–R565. https://doi.org/10.1016/j.cub.2019.05.019

Quinn, G. P., & Keough, M. J. (2023a). Simple Linear Models with One Predictor. In G. P. Quinn & M. J. Keough (Eds.), *Experimental Design and Data Analysis for Biologists* (2nd ed., pp. 76–114). Cambridge University Press. https://doi.org/DOI: 10.1017/9781139568173.007

Quinn, G. P., & Keough, M. J. (2023b). Introduction to Linear Models. In G. P. Quinn & M. J. Keough (Eds.), *Experimental Design and Data Analysis for Biologists* (2nd ed., pp. 45–61). Cambridge University Press. https://doi.org/DOI: 10.1017/9781139568173.005

R Core Team. (2024). *R: A Language and Environment for Statistical Computing*. https://www.R-project.org/

Ram, K., & Wickham, H. (2023). *wesanderson: A Wes Anderson Palette Generator*. https://CRAN.R-project.org/package=wesanderson

Rhoades, D. F. (1979). Evolution of plant chemical defenses against herbivores. In G. A. Rosenthal & D. H. Janzen (Eds.), *Herbivores: Their interaction with secondary plant metabolites. Academic press* (pp. 3–54).

Riegman, R., Boer, M. de, & Domis, L. de S. (1996). Growth of harmful marine algae in multispecies cultures. *Journal of Plankton Research*, *18*(10), 1851–1866. https://doi.org/10.1093/plankt/18.10.1851

Rigby, K., Berdalet, E., Berglund, C., Roger, F., Steinke, M., Saha, M., Grebner, W., Brown, E., John, U., Gamfeldt, L., Fink, P., Berggren, F., & Selander, E. (2024). Direct and indirect effects of copepod grazers on community structure. *Journal of Plankton Research*, *46*(5), 515–524. https://doi.org/10.1093/plankt/fbae047

Ritz, C., Baty, F., Streibig, J. C., & Gerhard, D. (2015). Dose-Response Analysis Using R. *PLOS ONE*, *10*(12), e0146021. https://doi.org/10.1371/journal.pone.0146021

Robinson, D., Hayes, A., & Couch, S. (2024). *broom: Convert Statistical Objects into Tidy Tibbles*. https://broom.tidymodels.org/

Ruxton, G. D., & Beauchamp, G. (2008). Time for some a priori thinking about post hoc testing. *Behavioral Ecology*, *19*(3), 690–693. https://doi.org/10.1093/beheco/arn020

643 Ryderheim, F., Selander, E., & Kiørboe, T. (2021). Predator-induced defence in a dinoflagellate
644 generates benefits without direct costs. *The ISME Journal, 15*(7), 2107–2116.
645 https://doi.org/10.1038/s41396-021-00908-y
646 Sailley, S. F., Polimene, L., Mitra, A., Atkinson, A., & Allen, J. I. (2015). Impact of zooplankton
647 food selectivity on plankton dynamics and nutrient cycling. *Journal of Plankton Research*,
648 *37*(3), 519–529. https://doi.org/10.1093/plankt/fbv020
649 Schindelin, J., Arganda-Carreras, I., Frise, E., Kaynig, V., Longair, M., Pietzsch, T., Preibisch,
650 S., Rueden, C., Saalfeld, S., Schmid, B., Tinevez, J.-Y., White, D. J., Hartenstein, V.,
651 Eliceiri, K., Tomancak, P., & Cardona, A. (2012). Fiji: an open-source platform for
652 biological-image analysis. *Nature Methods*, *9*(7), 676–682.
653 https://doi.org/10.1038/nmeth.2019
654 Selander, E., Thor, P., Toth, G., & Pavia, H. (2006). Copepods induce paralytic shellfish toxin
655 production in marine dinoflagellates. *Proceedings of the Royal Society B: Biological*
656 *Sciences*, *273*(1594), 1673–1680. https://doi.org/10.1098/rspb.2006.3502
657 Selander, E., Jakobsen, H. H., Lombard, F., & Kiørboe, T. (2011). Grazer cues induce stealth
658 behavior in marine dinoflagellates. *Proceedings of the National Academy of Sciences*,
659 *108*(10), 4030–4034. https://doi.org/10.1073/pnas.1011870108
660 Selander, E., Fagerberg, T., Wohlrab, S., & Pavia, H. (2012). Fight and flight in dinoflagellates?
661 Kinetics of simultaneous grazer-induced responses in *Alexandrium tamarense*. *Limnology*
662 *and Oceanography*, *57*(1), 58–64. https://doi.org/10.4319/lo.2012.57.1.0058
663 Selander, E., Kubanek, J., Hamberg, M., Andersson, M. X., Cervin, G., & Pavia, H. (2015).
664 Predator lipids induce paralytic shellfish toxins in bloom-forming algae. *Proceedings of the*

National Academy of Sciences, *112*(20), 6395–6400. https://doi.org/10.1073/pnas.1420154112

Selander, E., Heuschele, J., Nylund, G. M., Pohnert, G., Pavia, H., Bjærke, O., Pender-Healy, L. A., Tiselius, P., & Kiørboe, T. (2016). Solid phase extraction and metabolic profiling of exudates from living copepods. *PeerJ*, *4*, e1529. https://doi.org/10.7717/peerj.1529

Selander, E., Berglund, E. C., Engström, P., Berggren, F., Eklund, J., Harðardóttir, S., Lundholm, N., Grebner, W., & Andersson, M. X. (2019). Copepods drive large-scale trait-mediated effects in marine plankton. *Science Advances*, *5*(2). https://doi.org/10.1126/sciadv.aat5096

Signorell, A. (2025). *DescTools: Tools for Descriptive Statistics*. https://github.com/andrisignorell/desctools

Singmann, H., Bolker, B., Westfall, J., Aust, F., & Ben-Shachar, M. S. (2024). *afex: Analysis of Factorial Experiments*. https://CRAN.R-project.org/package=afex

Smayda, T. J. (1997). Harmful algal blooms: Their ecophysiology and general relevance to phytoplankton blooms in the sea. *Limnology and Oceanography*, *42*(5part2), 1137–1153. https://doi.org/10.4319/lo.1997.42.5_part_2.1137

Smayda, T. J. (2002). Adaptive Ecology, Growth Strategies and the Global Bloom Expansion of Dinoflagellates. *Journal of Oceanography*, *58*(2), 281–294. https://doi.org/10.1023/A:1015861725470

Smayda, T. J., & Reynolds, C. S. (2003). Strategies of marine dinoflagellate survival and some rules of assembly. *Journal of Sea Research*, *49*(2), 95–106. https://doi.org/10.1016/S1385-1101(02)00219-8

687 Stamp, N. (2003). Out Of The Quagmire Of Plant Defense Hypotheses. *The Quarterly Review of*
688 *Biology*, *78*(1), 23–55. https://doi.org/10.1086/367580
689 Turner, J. (2004). The importance of small planktonic copepods and their roles in pelagic marine
690 food webs. *Zoological Studies*, *42*(2).
691 Valiadi, M., & Iglesias-Rodriguez, D. (2013). Understanding Bioluminescence in
692 Dinoflagellates—How Far Have We Come? *Microorganisms*, *1*(1), 3–25.
693 https://doi.org/10.3390/microorganisms1010003
694 White, H. H. (1979). Effects of dinoflagellate bioluminescence on the ingestion rates of
695 herbivorous zooplankton. *Journal of Experimental Marine Biology and Ecology*, *36*(3),
696 217–224. https://doi.org/10.1016/0022-0981(79)90117-5
697 Wickham, H. (2016). *ggplot2: Elegant Graphics for Data Analysis*. Springer-Verlag New York.
698 https://ggplot2.tidyverse.org
699 Wickham, H., Averick, M., Bryan, J., Chang, W., McGowan, L. D., François, R., Grolemund,
700 G., Hayes, A., Henry, L., Hester, J., Kuhn, M., Pedersen, T. L., Miller, E., Bache, S. M.,
701 Müller, K., Ooms, J., Robinson, D., Seidel, D. P., Spinu, V., … Yutani, H. (2019).
702 Welcome to the Tidyverse. *Journal of Open Source Software*, *4*(43), 1686.
703 https://doi.org/10.21105/joss.01686
704 Wickham, H., & Bryan, J. (2023). *readxl: Read Excel Files*. https://readxl.tidyverse.org,
705 https://github.com/tidyverse/readxl
706 Wilke, C. O., & Wiernik, B. M. (2022). *ggtext: Improved Text Rendering Support for "ggplot2."*
707 https://CRAN.R-project.org/package=ggtext
708

Wilke, C. O. (2024). *cowplot: Streamlined Plot Theme and Plot Annotations for "ggplot2."* https://wilkelab.org/cowplot/

Yamamoto, T., & Tarutani, K. (1999). Growth and phosphate uptake kinetics of the toxic dinoflagellate Alexandrium tamarense from Hiroshima Bay in the Seto Inland Sea, Japan. *Phycological Research*, *47*(1), 27–32. https://doi.org/10.1046/j.1440-1835.1999.00149.x

Yu, G. (2023). *ggimage: Use Image in "ggplot2."* https://CRAN.R-project.org/package=ggimage

Zhu, H. (2024). *kableExtra: Construct Complex Table with "kable" and Pipe Syntax*. https://CRAN.R-project.org/package=kableExtra

Data availability

The data supporting this study is available in Zenodo at https://doi.org/10.5281/zenodo.14883074.

Supporting information

Grazer-induced bioluminescence and toxicity in marine dinoflagellates

Paula Gonzalo-Valmala[1](ORCID: 0009-0005-4270-4860)**, Milad Pourdanandeh**[2] (ORCID: 0009-0002-7640-5728), **Sandra Lage**[3] (ORCID: 0000-0003-0167-7163)**, Erik Selander**[1*] (ORCID: 0000-0002-2579-0841)

[1] Department of Biology, Lund University, Lund, Sweden

[2] Department of Marine Sciences, University of Gothenburg, Gothenburg, Sweden

[3] Centre of Marine Sciences (CCMAR/CIMAR LA), University of Algarve, Faro, Portugal

*** Correspondence:**

Name: Erik Selander

E-mail: erik.selander@biol.lu.se

Running head: Grazer-induced responses in marine dinoflagellates

Keywords: Marine dinoflagellates, Inducible defenses, Copepods, Copepodamides, Bioluminescence, Harmful algae, Paralytic shellfish toxins

Table S1: Composition of individual copepodamide congeners in the purified copepodamide extract used. Congeners lacking a fatty acid group (NA) are deacylated scaffolds. Sum of copepodamides = 29.9 µM.

Scaffold	Fatty acid	*m/z* precursor ion	Concentration (µM)
Copepodamides (*m/z* product ion: 430)	NA	448.3	0.030
	14:0 (Myritic)	658.5	0.522
	16:0 (Palmitic)	686.5	1.561
	18:4 (Stearidonic)	706.5	2.832
	20:5 (Eicosapentaenoic)	732.5	5.007
	22:6 (Cervonic)	758.6	18.41
Dihydro-copepodamides (*m/z* product ion: 432)	NA	450.3	0.002
	18:4 (Stearidonic)	708.5	0.236
	20:5 (Eicosapentaenoic)	734.5	0.330
	22:6 (Cervonic)	760.5	0.961

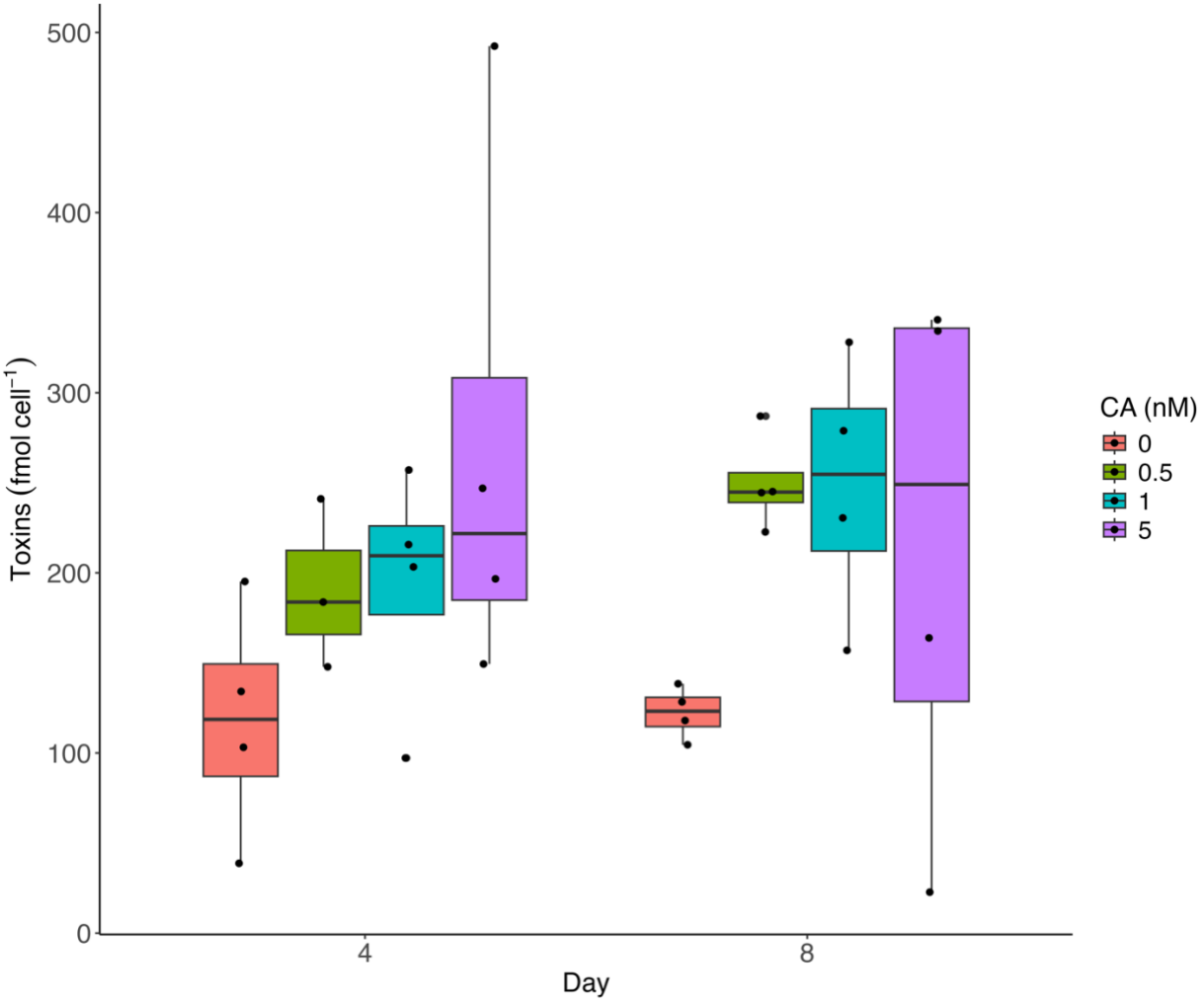

Fig. S1 Boxplot showing the levels of paralytic shellfish toxins (fmol cell^{-1}) produced by *Alexandrium catenella* on days 4 and 8 across different copepodamide concentrations (0-0.5-1-5 nM).